ECONOMIC GEOLOGY

AND THE

BULLETIN OF THE SOCIETY OF ECONOMIC GEOLOGISTS

VOL. 91 NOVEMBER, 1996 No. 7

Assessing Metasomatic Mass and Volume Changes Using the Bootstrap, with Application to Deep Crustal Hydrothermal Alteration of Marble

JAY J. AGUE AND JOOST L. M. VAN HAREN*

Department of Geology and Geophysics, Yale University, P.O. Box 208109, New Haven, Connecticut 06520-8109

Abstract

A statistically rigorous approach for determining likely errors on estimates of mass and volume change in metasomatic systems is presented and then used to assess mass transfer resulting from hydrothermal alteration of marble during regional metamorphism. Analysis of metasomatic effects using standard statistical methods designed for unconstrained, univariant data often fails to provide useful results for several important reasons:

1. The concentration of any constituent in a composition is constrained to be between 0 and 100 wt percent.
2. The sum of the concentrations of all constituents must be 100 wt percent (the closure constraint). Compositions are multivariate and provide information only about the relative proportions of constituents.
3. The maximum possible mass or volume loss is −100 percent (−100% corresponds to complete mass or volume loss).
4. Rock bulk density must be greater than 0 g cm^{-3}.
5. The underlying probability distributions for mass and volume changes are commonly non-normal.

To address these issues, we use statistical procedures recently developed to treat the special properties of compositional data, including closure, and the bootstrap method to compute accurate confidence intervals for assessing how far in error best estimates of mass and volume change are likely to be. The bootstrap deals effectively with non-normality and constraints (1), (3), and (4).

We apply our approach to gain a better understanding of synmetamorphic (Acadian orogeny) hydrothermal alteration of upper greenschist facies and amphibolite facies marble beds of the Wepawaug Schist, Connecticut. The marbles lost significant amounts of volatiles (dominantly CO_2 and H_2O), Si, Ti, K, Rb, Sr, and Ba. Best estimates of total mass and volume change are −27 and −32 percent, respectively. The bulk of the lost mass was volatiles (~140 g kg^{-1}), SiO_2 (~60 g kg^{-1}), and K_2O (~15 g kg^{-1}) (numbers are g lost per kg of parent rock). Volatile loss was probably regional in scope. Loss of Si, Ti, K, Rb, Sr, and Ba occurred over minimum length scales on the order of typical hand sample dimensions; maximum length scales remain to be determined.

The FORTRAN 77 computer code that performs the calculations described herein is available from the senior author.

Introduction

A BASIC requirement for understanding any metasomatic process is to determine the amounts of volume strain and gains and losses of chemical constituents resulting from fluid-rock interaction. Element mobility is a function of many fundamental geologic variables including temperature, pressure, reaction kinetics, rock composition, and the composition and amount of infiltrating fluid. Consequently, careful evaluation of mass transfer systematics can place critical constraints on fluid/rock ratios and fluid fluxes, directions of fluid motion relative to temperature and pressure gradients, fluid-rock disequilibrium and time scales of fluid flow, and fluid sources and flow paths. Mass and volume change are genetically linked in open systems and, thus, studies of metasomatism must consider both rock physical and chemical properties (e.g., Brimhall and Dietrich, 1987; Brimhall et al., 1988).

Investigation of metasomatic mass and volume changes generally requires statistical analysis because of (1) heterogeneities in the compositions of parent rocks, (2) differing types and extents of chemical and volume change in the altered rocks, and (3) analytical errors. Statistical analysis is made difficult, however, by a variety of factors which, in spite of their importance are rarely considered in studies of mass and volume change. For example, the concentrations of constituents in a composition are governed by two basic constraints. First, concentration values are bounded between 0 and 100 wt %. Second, the concentration sum for all constituents must be 100 wt % (the closure constraint). Compositions are inherently multivariate and provide information only about the relative, not the absolute, amounts of constituents. As shown by Chayes (1960) and Aitchison (1986), for example, standard statistical procedures that ignore the special proper-

* Present address: Biosphere 2 Center, Inc., P.O. Box 689, Oracle, Arizona 85623.

0361-0128/96/1864/1169-14$5.00

ties of compositional data often yield misleading or erroneous results. The values that mass and volume changes can take are also constrained because the maximum possible mass or volume loss is −100% (−100% corresponds to complete mass or volume loss). Furthermore, rock bulk densities must be greater than 0 g cm^{-3}. An additional major problem is that the statistical methods in common use are based on the normal (Gaussian) distribution, but underlying probability distributions in mass and volume change problems can be highly non-normal.

To address these issues, we present a statistically rigorous approach for analysis of mass and volume changes in metasomatic systems. Our approach has two key components: (1) mean compositions are computed using the recently developed statistical procedures of Aitchison (1986, 1989) which take full account of the special properties of compositional data, including closure; and (2) assessment of how far in error the best estimates of mass and volume change are likely to be is made using the bootstrap method. The bootstrap, introduced by Efron (1979), is another recent development in statistics. Our bootstrap application deals effectively with non-normal distributions and the constraints on the values of mass and volume change, bulk density, and concentrations of individual chemical constituents. Ague (1994a) used the bootstrap in conjunction with the methods of Aitchison (1986, 1989) to estimate standard errors for volume strain and total rock mass change. Here, we extend this treatment and compute accurate confidence intervals for volume strain, total mass change, and the mass changes of individual constituents using calibration of bootstrap percentile intervals (cf. Efron, 1979; Hall, 1987; Loh, 1987; Efron and Tibshirani, 1993).

We use our approach to obtain a better understanding of mass and volume changes that resulted when marble beds of the Wepawaug Schist, Connecticut, underwent hydrothermal alteration during regional metamorphism. Previous petrologic and isotopic studies have demonstrated that regional metamorphic belts develop as dynamic hydrothermal systems, but considerable controversy remains regarding the pathways, scales, amounts, and timing of fluid flow, and the related issues of advective heat and mass transfer (e.g., Brady, 1988; Chamberlain and Rumble, 1988; Hoisch, 1991; Ferry, 1992; Ague, 1994a, 1994b; Moss et al., 1995). Whether or not fluids can transport significant quantities of "non-volatile" elements into and out of rocks remains as perhaps the most controversial question in the debate. If considerable non-volatile element transport occurs, then rocks cannot be treated as "isochemical" systems, regardless of whether the scale of transport is over centimeters or kilometers. Clearly, if fluid-driven mass transfer of non-volatile elements is regional in scale, then metamorphic processes play a significant but, as yet, poorly understood role in the geochemical cycling of ore metals and other elements both within the Earth's crust and between the crust and the shallow hydrosphere. Our focus is on metamorphic mass transfer and volume strain, but our methods are applicable to any type of metasomatic system.

Review of Mass Balance Equations

Because the equations describing mass and volume change in open systems have been discussed extensively elsewhere (cf. Gresens, 1967; Grant, 1986; Brimhall and Dietrich, 1987; Brimhall et al., 1988; Ague, 1994a), only a brief review is given here. The basic task is to quantify mass and volume changes in metasomatically altered rock relative to the parent rock or protolith. The results provide information about the time integrated effects of all metasomatism that a given altered rock or suite of altered rocks has undergone.

The total change in mass resulting from metasomatism, T, is (cf. Ague, 1994a):

$$\left[\frac{\text{final mass} - \text{initial mass}}{\text{initial mass}}\right] = \left[\frac{C_i^\circ}{C_i'} - 1\right], \qquad (1)$$

where C_i° and C_i' are the concentrations of a reference immobile species i in the parent rock and the altered rock, respectively (all symbols are listed in Table 1). For example, a total mass change of −0.5 (or −50%) means that 1 kg of parent rock lost 500 g during alteration. Positive mass change values indicate overall mass gain.

Volume strain, ϵ, results from mass loss or gain and changes in bulk density:

$$\left[\frac{\text{final volume} - \text{initial volume}}{\text{initial volume}}\right] = \left[\left(\frac{C_i^\circ}{C_i'}\right)\left(\frac{\rho^\circ}{\rho'}\right) - 1\right], \qquad (2)$$

where ρ° and ρ' are the bulk densities of the parent and altered rocks, respectively. Equation (2) gives the overall amount of volume strain, but provides no direct information about the directions of shape change. Negative volume strains

TABLE 1. List of Symbols

B	= total number of bootstrap samples
C, c	= concentration (wt % or ppm)
g	= geometric mean
mr	= geometric mean reference ratio
M	= total number of chemical species
N	= total number of samples
r	= protolith/altered concentration ratio
$s(\cdot)$	= function
T	= total mass change
AML	= Aitchison measure of location (eq 5)
D	= matrix of concentrations and bulk densities
α	= used to specify confidence limits
ϵ	= volume strain
θ	= general symbol for a parameter
ρ	= bulk-rock density ([M][L^{-3}])
ρ_g	= grain density ([M][L^{-3}])
$\hat{\sigma}_{se}$	= estimated standard error
τ^j	= mass change for mobile species j

Accents, subscripts, and superscripts

$\hat{}$	= estimate
$\bar{}$	= mean or measure of location
i	= reference (immobile) species index
j	= mobile species index
m	= general (mobile or immobile) species index
n	= sample index
$\%,lo$	= lower confidence point for percentile interval
$\%,hi$	= upper confidence point for percentile interval
Σ	= sum of reference species concentrations
$^\circ$	= protolith or parent rock
$'$	= altered rock
*	= bootstrap sample, bootstrap replicate

indicate volume loss, whereas positive strains indicate volume gain.

The total mass change reflects the mass changes of each mobile constituent j. The mass change for a mobile constituent, τ^j (Brimhall et al., 1989), is:

$$\left[\frac{\text{final mass } j - \text{initial mass } j}{\text{initial mass } j}\right] = \frac{\rho'}{\rho^\circ}\frac{C_j'}{C_j^\circ}(\epsilon + 1) - 1, \quad (3)$$

where C_j° and C_j' are the concentrations of j in the parent and altered rocks, respectively. Equation 3 expresses mass changes for j in terms of rock chemical, physical, and volumetric properties. It may be simplified, however, by substituting the right side of equation 2 for the ϵ term:

$$\left[\frac{\text{final mass } j - \text{initial mass } j}{\text{initial mass } j}\right] = \left[\left(\frac{C_i^\circ}{C_i'}\right)\left(\frac{C_j'}{C_j^\circ}\right) - 1\right]. \quad (4)$$

A negative τ^j value indicates mass loss of j; a positive value indicates mass gain.

Complexitites of Compositional Data: Some Examples

The concentrations of chemical constituents in a composition are governed by two basic constraints. First, the concentration of any constituent cannot be less than 0 wt percent or greater than 100 wt percent. Second, compositions are subject to closure such that the constituents must sum to 100 wt percent. These constraints seem obvious enough, but they pose special problems for mass balance and statistical analysis that are rarely considered in studies of metasomatism. Two simple examples are presented below to highlight these problems; the reader is referred to Aitchison (1986) and Woronow and Love (1990) for comprehensive discussions of the properties of compositional data.

Bounded concentrations

The fact that the concentration of any constituent is bounded between 0 and 100 wt percent can cause problems for typical statistical analysis methods. Take, for instance, the sample standard deviation, which is commonly used to describe the inherent variability of an element's or oxide's concentration in a suite of compositions. As a concrete example, consider the K_2O content of hydrothermally altered marbles from the Wepawaug Schist, Connecticut (Table 2; this data set will be discussed in more detail below). The mean ± 2 sample standard deviations ($\pm 2\sigma$) is 0.58 $\pm$ 1.20 wt percent, which implies that K_2O concentrations extend to negative values. Of course, negative concentrations are impossible. This simple example shows, therefore, that sample standard

TABLE 2. Chemical Analyses

Sample no.	Cal-ank-ms marbles							Altered marbles					
	27	28	32	36	37	38	39	16	24A	34	35	119B	W6B
Weight percent													
SiO_2	26.80	29.00	28.70	24.40	31.30	27.90	28.80	33.00	25.60	26.60	32.00	36.50	24.70
TiO_2	0.22	0.31	0.31	0.30	0.20	0.17	0.21	0.30	0.26	0.22	0.25	0.32	0.22
Al_2O_3	5.72	7.43	7.61	7.11	4.78	4.26	5.02	7.39	6.18	6.46	8.22	8.40	5.19
Fe_2O_3	2.44	4.08	4.08	4.61	2.93	2.80	2.78	4.29	4.19	3.93	4.68	6.23	5.64
MgO	2.12	5.53	3.08	3.17	5.71	6.15	4.89	5.27	7.29	5.04	5.67	6.14	4.69
MnO	0.34	0.29	0.29	0.41	0.25	0.21	0.19	0.43	0.36	0.36	0.42	0.42	0.60
CaO	32.60	26.20	28.70	28.70	26.30	28.20	28.50	31.70	32.70	35.80	33.00	29.80	32.20
Na_2O	0.11	0.69	0.13	0.20	0.26	0.18	0.22	0.25	0.16	0.17	0.24	0.20	0.24
K_2O	1.81	1.56	1.98	2.15	1.26	1.25	1.51	1.22	1.28	0.11	0.04	0.01	0.80
P_2O_5	0.15	0.12	0.16	0.25	0.12	0.13	0.15	0.18	0.23	0.17	0.31	0.26	0.36
L.O.I.	27.90	24.50	24.30	27.70	27.20	28.90	27.40	14.60	20.30	19.80	14.60	12.00	24.80
Total	100.39	99.84	99.51	99.18	100.47	100.32	99.86	98.76	98.74	99.79	99.56	100.36	99.56
Parts per million (element)													
Rb	63	46	49	70	43	43	44	30	63	5.90	2.68	0.54	43
Sr	1,170	635	941	1,180	925	1,080	1,300	662	1,170	920	823	427	719
Ba	201	257	270	161	217	186	171	226	172	37.93	5.69	0.14	68
Zr	20	59	49	34	38	23	24	57	55	31	35	51	39
Zn	70	52	52	49	45	43	48	60	51	65	131	73	50
Ni	16	26	20	29	17	12	18	24	28	13	25	34	37
Nb	17	15	18	12	17	12	17	15	22	21	22	19	23
Co	7	9	7	10	11	7	9	9	7	8	16	16	17
ρ_g	2.74	2.84	2.77	2.82	2.80	2.79	2.77	3.01	2.94	2.97	3.09	3.17	2.85
Zone	Grt	Grt	St	Chl	Chl	Chl	Chl	Ky	Grt	Ky	Ky	Ky	Ky

All Fe as Fe_2O_3
L.O.I. = loss on ignition, ρ_g = grain density (g cm^{-3})
Weight percent totals include trace elements summed as oxides
Mineral abbreviations: Cal = calcite, Ank = ankerite, Ms = muscovite
Metamorphic zones: Grt = garnet, St = staurolite, Chl = chlorite, Ky = kyanite

deviation calculations, when applied uncritically, can yield results that are worthless as quantitative measures of compositional variability.

Closure

From as early as the late nineteenth century it has been recognized that the closure constraint must be considered when assessing relationships among compositional variables (cf. Pearson, 1897; Chayes, 1960). This task has proven to be difficult, but the landmark theoretical work of Aitchison (e.g., Aitchison, 1986) has made rigorous analysis possible. Our purpose here is to provide a simple illustration of the importance of closure in the context of mass balance.

Consider a hypothetical quartzite with composition SiO_2 = 99.2 wt percent, TiO_2 = 0.72 wt percent, and ZrO_2 = 0.08 wt percent. Suppose that 100 kg of this rock loses 20 kg of SiO_2 as a result of some mass transfer process. The mass of silica has therefore decreased from 99.2 to 79.2 kg; the masses of TiO_2 and ZrO_2 remain unchanged. To form a composition for the altered rock, the masses of the various oxides must be normalized to 100 wt percent. Thus, the composition of the altered rock is SiO_2 = 99.0 wt percent, TiO_2 = 0.90 wt percent, and ZrO_2 = 0.10 wt percent. Surprisingly, even though the rock has lost 20 percent of its silica mass, the concentration of silica has decreased by only 0.2 wt percent (e.g., from 99.2 to 99.0 wt %)! Furthermore, the concentrations of TiO_2 and ZrO_2 have increased, but no mass transfer involving these oxides has occurred. Clearly, closure has the potential to obscure seriously the effects of mass transfer. As a result, wt percents, in and of themselves, provide no direct information about the nature and magnitude of elemental gains and losses. Moreover, the example shows that compositional data are inherently multivariate, that is, the concentrations of all the constituents are related to each other by the process of closure. It is worth noting in this regard that the concentrations of trace constituents are commonly assumed to be largely immune from the effects of closure. The above example shows, however, that such assumptions are incorrect. The concentration of the trace constituent ZrO_2 increases by the same relative amount as that of TiO_2 when the oxide masses in the altered rock are normalized to sum to 100 wt percent.

Problems with Averaging Compositional Data

A fundamental question that many studies of metasomatic processes address is how much compositional and volumetric change has the average altered rock undergone relative to the average protolith? The averages are typically calculated using standard arithmetic means, which are designed for univariant, unconstrained data. Such calculations are straightforward but can lead to misleading or erroneous conclusions because compositions contain information only about the relative, not the absolute, proportions of constituents; and are constrained by closure. Consequently, computations should be done using the ratios of constituents in a multivariate way (Aitchison, 1986, 1989).

Aitchison (1989) proposed a method for computing a representative mean composition (or measure of location) that uses a multivariate treatment of compositional ratios and avoids the problems of traditional statistical analysis. The details of the theory behind this method are beyond the scope of this paper; our focus, therefore, is on the end result (see Aithchison 1989, and Woronow and Love, 1990, for further discussion). The measure of location for the data set is expressed in vector form as:

$$(\bar{C}_1, \bar{C}_2, \ldots, \bar{C}_M) = \frac{(g_1, g_2, \ldots, g_M)}{0.01 \sum_{m=1}^{M} g_m}, \quad (5)$$

where $\bar{C}_m$ is the concentration of constituent m (the factor of 0.01 converts to wt %) and M is the total number of constituents; g_m denotes the geometric mean concentration of constituent m:

$$g_m = \exp\left[N^{-1} \sum_{n=1}^{N} \ln (c_{n,m})\right], \quad (6)$$

where $c_{n,m}$ is the concentration of m in sample n and N is the total number of samples. The normalization to 100 wt percent in equation 5 is of key importance because it forms a composition by relating the geometric means of all of the constituents to each other through the process of closure. Throughout this paper, a composition vector computed using equation 5 is referred to as an "AML," which is an abbreviation for Aitchison measure of location.

Bulk Density

Mean bulk densities for the protolith and altered rock suites are required to estimate volume changes (eqn 2). The standard arithmetic mean:

$$\bar{\rho} = N^{-1} \sum_{n=1}^{N} \rho_n, \quad (7)$$

is satisfactory for most problems ($\bar{\rho}$ = mean bulk density; ρ_n = bulk density of sample n). Bulk density must be greater than 0 g cm^{-3}. Because most rocks are relatively dense ($\rho >$ ~2 g cm^{-3}), this constraint is rarely problematic in practice.

Bootstrap Statistics for Mass Balance Problems

Estimates of mass and volume change are subject to uncertainties relating to density and composition heterogeneities in the protolith, differing types and extents of metasomatic alteration reactions, and analytical uncertainties. This physicochemical variability commonly necessitates use of statistical methods to determine whether estimated mass and volume changes differ from zero at a statistically significant level; and what the minimum detectable amounts of mass and volume change are for the system. These determinations are generally made using methods assuming that samples come from populations having approximately normal (Gaussian) relative frequency distributions. If, however, the underlying distributions deviate substantially from the normal case, then statistical analysis can be compromised severely. Moreover, aside from a handful of studies (e.g., Woronow and Love, 1990; Ague, 1994a), the statistical treatments in common use do not account for the special constraints on compositions, such as closure.

The nonparametric bootstrap method, introduced by Efron (1979), is a Monte Carlo statistical analysis technique that is

free from assumptions about underlying distributions. The power of the bootstrap is that it uses the data set at hand as the estimator of the underlying distributions. Furthermore, the bootstrap can assess standard errors and confidence limits for virtually any statistic, even those for which closed-form analytical solutions are unavailable. This section focuses specifically on the bootstrap method in relation to mass balance problems; the reader is referred to the excellent book by Efron and Tibshirani (1993) for a comprehensive review of the method and its applications.

Resampling strategy for mass balance problems

Data analysis problems often boil down to estimating some parameter of interest, θ, using some function of the observed data, $s(\mathbf{x})$:

$$\hat{\theta} = s(\mathbf{x}), \tag{8}$$

where $\hat{\theta}$ is the estimate and $\mathbf{x}$ is a random sample from an unknown probability distribution. Having made the estimate, we then want a measure of its statistical accuracy (in other words, we want a reasonable idea of how far in error $\hat{\theta}$ might be). The bootstrap was designed for this task. Bootstrap analysis proceeds by random resampling of the original data sets with replacement in order to form a large number, B, of synthetic data sets, or "bootstrap samples," $\mathbf{x}^*$. Take, for example, $\mathbf{x}$ to be a data set of four numbers: (x_1, x_2, x_3, x_4). The first few bootstrap samples might be $\mathbf{x}^{*1} = (x_1, x_1, x_3, x_2)$, $\mathbf{x}^{*2} = (x_2, x_2, x_2, x_4)$, $\mathbf{x}^{*3} = (x_2, x_4, x_1, x_1)$, and so on. Note that for any given bootstrap sample, some of the original observations can be absent, and any observation can occur more than once. A bootstrap replicate, $\hat{\theta}^*$, is then computed for each of the bootstrap samples:

$$\hat{\theta}^* = s(\mathbf{x}^*). \tag{9}$$

If $s(\mathbf{x})$ is the mean, then $\hat{\theta}^{*1} = s(\mathbf{x}^{*1}) = (x_1 + x_1 + x_3 + x_2)/4$. The final part of the analysis is to assess the most likely errors on the estimate of θ directly using the full population of replicates. Statistical model assumptions are, therefore, unnecessary in the analysis.

Bootstrap sample and replicate principles are readily extendible to problems of mass and volume change. The measured rock compositions and bulk densities are best treated as a $(N^\circ + N') \times (M + 1)$ data matrix, $\mathbf{D}$:

$$\mathbf{D} = \begin{pmatrix} c^\circ_{1,1} & c^\circ_{1,2} & \cdots & c^\circ_{1,M} & \rho^\circ_1 \\ c^\circ_{2,1} & c^\circ_{2,2} & \cdots & c^\circ_{2,M} & \rho^\circ_2 \\ \vdots & \vdots & \cdots & \vdots & \vdots \\ c^\circ_{N^\circ,1} & c^\circ_{N^\circ,2} & \cdots & c^\circ_{N^\circ,M} & \rho^\circ_{N^\circ} \\ c'_{1,1} & c'_{1,2} & \cdots & c'_{1,M} & \rho'_1 \\ c'_{2,1} & c'_{2,2} & \cdots & c'_{2,M} & \rho'_2 \\ \vdots & \vdots & \cdots & \vdots & \vdots \\ c'_{N',1} & c'_{N',2} & \cdots & c'_{N',M} & \rho'_{N'} \end{pmatrix}, \tag{10}$$

where N° and N' are the numbers of protolith and altered rock samples, respectively. The protolith compositions and bulk densities form the first N° rows of $\mathbf{D}$ (one sample per row), and the altered rock data forms the remaining N' rows. Each of the first M columns corresponds to a chemical constituent in the composition; column 1 could be SiO_2, column 2 TiO_2, etc. The final column holds the bulk densities for all samples. The protolith and altered rock suites are assumed to be mutually independent random samples from unknown probability distributions.

The **AML** composition vector for the protolith suite is constructed from the first N° rows and M columns of $\mathbf{D}$ using equation 5, yielding:

$$\mathbf{AML}^\circ = (\bar{C}^\circ_1, \bar{C}^\circ_2, \ldots, \bar{C}^\circ_M). \tag{11}$$

Likewise, the **AML** vector for the altered rock suite is constructed from the last N' rows of $\mathbf{D}$:

$$\mathbf{AML}' = (\bar{C}'_1, \bar{C}'_2, \ldots, \bar{C}'_M). \tag{12}$$

Using these **AML**'s, best estimates (also referred to as "point estimates") of mass change are calculated:

$$\hat{T} = \left(\frac{\bar{C}^\circ_i}{\bar{C}'_i}\right) - 1, \tag{13}$$

and

$$\hat{\tau}^j = \left(\frac{\bar{C}^\circ_i}{\bar{C}'_i}\right)\left(\frac{\bar{C}'_j}{\bar{C}^\circ_j}\right) - 1. \tag{14}$$

Arithmetic mean bulk densities for the protolith and altered suites ($\bar{\rho}^\circ$, $\bar{\rho}'$) are computed using the $\rho^\circ_1 \ldots \rho^\circ_{N^\circ}$ and $\rho'_1 \ldots \rho'_{N'}$ entries in the last column of $\mathbf{D}$, respectively. The best estimate of volume change based on the **AML** compositions and the arithmetic mean densities is thus:

$$\hat{\epsilon} = \left(\frac{\bar{C}^\circ_i}{\bar{C}'_i}\right)\left(\frac{\bar{\rho}^\circ}{\bar{\rho}'}\right) - 1. \tag{15}$$

The bootstrap analysis uses populations of replicate $\hat{T}$, $\hat{\tau}^j$, and $\hat{\epsilon}$ values to estimate errors on calculated mass and volume changes (symbols for replicates are $\hat{T}^*$, $\hat{\tau}^{j*}$, and $\hat{\epsilon}^*$). A bootstrap sample constructed from $\mathbf{D}$, denoted as $\mathbf{D}^*$, is also a $(N^\circ + N') \times (M + 1)$ matrix. The first N° rows of $\mathbf{D}^*$ are resampled from the protolith specimens and the remaining N' rows are resampled from the altered rock specimens. For example, consider a suite of four protolith samples ($N^\circ = 4$) and four altered samples ($N' = 4$) in a chemical system composed of four constituents ($M = 4$). Suppose a bootstrap resampling iteration selects samples 1, 4, 2, and 2 from the protolith suite and samples 3, 1, 1, and 1 from the altered suite. The resulting bootstrap sample $\mathbf{D}^*$ matrix is:

$$\mathbf{D}^* = \begin{pmatrix} c^\circ_{1,1} & c^\circ_{1,2} & c^\circ_{1,3} & c^\circ_{1,4} & \rho^\circ_1 \\ c^\circ_{4,1} & c^\circ_{4,2} & c^\circ_{4,3} & c^\circ_{4,4} & \rho^\circ_4 \\ c^\circ_{2,1} & c^\circ_{2,2} & c^\circ_{2,3} & c^\circ_{2,4} & \rho^\circ_2 \\ c^\circ_{2,1} & c^\circ_{2,2} & c^\circ_{2,3} & c^\circ_{2,4} & \rho^\circ_2 \\ c'_{3,1} & c'_{3,2} & c'_{3,3} & c'_{3,4} & \rho'_3 \\ c'_{1,1} & c'_{1,2} & c'_{1,3} & c'_{1,4} & \rho'_1 \\ c'_{1,1} & c'_{1,2} & c'_{1,3} & c'_{1,4} & \rho'_1 \\ c'_{1,1} & c'_{1,2} & c'_{1,3} & c'_{1,4} & \rho'_1 \end{pmatrix}. \tag{16}$$

Note that because the same resampling indices are used for compositions and bulk densities, fundamental linkages between rock chemical and physical properties are preserved

for each $\mathbf{D}^*$ (e.g., Ague, 1994a). AML composition vectors for the protolith and altered rocks are constructed from each $\mathbf{D}^*$ using equation 5:

$$\mathbf{AML}^{\circ *} = (\bar{C}_1^{\circ *}, \bar{C}_2^{\circ *}, \ldots, \bar{C}_M^{\circ *}), \quad (17)$$

and

$$\mathbf{AML}'^{*} = (\bar{C}_1'^{*}, \bar{C}_2'^{*}, \ldots, \bar{C}_M'^{*}). \quad (18)$$

The replicate mass and volume changes are therefore:

$$\hat{T}^* = \left(\frac{\bar{C}_i^{\circ *}}{\bar{C}_i'^{*}}\right) - 1, \quad (19)$$

$$\hat{\tau}^{j*} = \left(\frac{\bar{C}_i^{\circ *}}{\bar{C}_i'^{*}}\right)\left(\frac{\bar{C}_j'^{*}}{\bar{C}_j^{\circ *}}\right) - 1, \quad (20)$$

and

$$\hat{\epsilon}^* = \left(\frac{\bar{C}_i^{\circ *}}{\bar{C}_i'^{*}}\right)\left(\frac{\bar{\rho}^{\circ *}}{\bar{\rho}'^{*}}\right) - 1, \quad (21)$$

where $\bar{\rho}^{\circ *}$ and $\bar{\rho}'^{*}$ are the replicate arithmetic mean bulk densities for parent and altered rock computed from the last column of $\mathbf{D}^*$.

In addition to the mass and volume change expressions, the ratios $\hat{r}_m = \bar{C}_m^{\circ}/\bar{C}_m'$, $m = 1 \ldots M$, are, in some cases, useful for assessing the geochemical reference frame (see below). Thus, for each bootstrap sample, the replicates:

$$\hat{r}_m^* = \frac{\bar{C}_m^{\circ *}}{\bar{C}_m'^{*}}, \quad m = 1 \ldots M, \quad (22)$$

are computed.

We emphasize that the above procedures take full account of the closure constraint and the multivariate nature of compositions by using equation 5 (the measure of location of Aitchison, 1989) to calculate the concentrations used for each bootstrap replication.

Much can often be learned from histograms of bootstrap replications. For example, a histogram of 5,000 bootstrap replications of the potassium mass change ($\hat{\tau}^{K_2O*}$) resulting from hydrothermal alteration of marbles of the Wepawaug Schist, Connecticut, is shown in Figure 1 (these rocks are discussed in detail in a later section). The bootstrap histogram is markedly non-normal, which strongly suggests that any statistical inferences about the potassium mass change based on the normal curve are suspect.

Confidence intervals

A powerful way to assess how far in error the best estimates for mass and volume change might be is to calculate confidence intervals for T, τ^j, and ϵ. For example, say that the 95 percent confidence interval for the total mass change, T, extends from −30 to −50 percent. This implies that one can be 95 percent confident that the true value of T lies between −30 and −50 percent.

The percentile interval, introduced by Efron (1979), is based on percentiles of the bootstrap distribution of a statistic and, therefore, is constructed directly from the real data sets

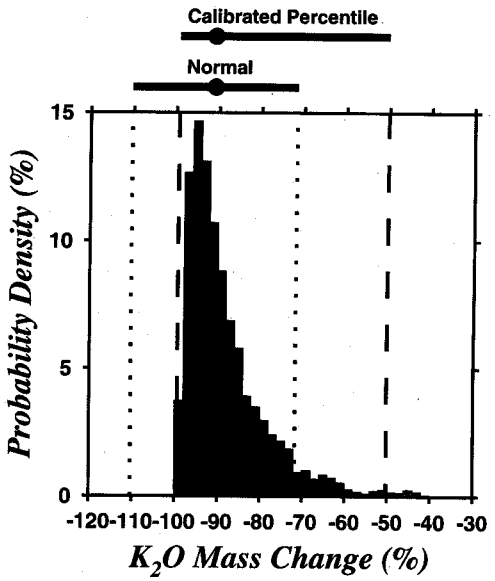

FIG. 1. Five thousand bootstrap replications of the K_2O mass change ($\hat{\tau}^{K_2O*}$) attending hydrothermal alteration of marbles from the Wepawaug Schist, Connecticut. Note that the histogram is markedly non-normal. The 95 percent confidence interval based on standard normal theory is denoted by vertical dotted lines; the 95 percent confidence interval calculated using the calibrated percentile method is denoted by vertical dashed lines; the best estimate of K_2O mass change ($\hat{\tau}^{K_2O}$) is denoted by filled circles. Note that the normal theory interval fails to capture the asymmetry of the distribution and extends to an impossible mass change value of −110 percent.

at hand. The lower and upper limits of the percentile interval for a parameter θ, denoted by $\hat{\theta}_{\%,lo}$ and $\hat{\theta}_{\%,hi}$, are closely approximated by (cf. Efron and Tibshirani, 1993, p. 171):

$$[\hat{\theta}_{\%,lo}, \hat{\theta}_{\%,hi}] \sim [\hat{\theta}_B^{*(\alpha)}, \hat{\theta}_B^{*(1-\alpha)}], \quad (23)$$

where B denotes that the interval is based on B bootstrap replications and α specifies the desired lower and upper limits (e.g., for a 95% confidence interval, $\alpha = 0.025$). The easiest way to proceed is first to sort all the replicates into ascending order. Then, $\hat{\theta}_B^{*(\alpha)}$ (which approximates $\hat{\theta}_{\%,lo}$) is given by the $B \cdot \alpha$th value in the sorted list. For example, if α is 0.025 and $B = 1{,}000$, then $\hat{\theta}_B^{*(\alpha)}$ is simply the $1{,}000 \cdot 0.025 = 25$th entry in the sorted list; $\hat{\theta}_{\%,hi}$ is approximated in an analogous way, using the $B \cdot (1 - \alpha\text{th})\hat{\theta}^*$ value in the sorted list.

Mass and volume change calculations involving small samples (small N°, N') can pose problems for the percentile interval. The problem that arises most commonly in practice is that confidence interval lengths (length = $\hat{\theta}_{\%,hi} - \hat{\theta}_{\%,lo}$) tend to be underestimated (cf. Efron and Tibshirani, 1993). One way to overcome the deficiencies of the percentile interval is to use bootstrap calibration. Calibration uses a second level of bootstrap resampling (a "nested" bootstrap) designed specifically to improve the accuracy of the lower and upper confidence points (Hall, 1987; Loh, 1987; Efron and Tibshirani, 1993). The details of the theory and calculation scheme for the calibration are beyond the scope of this paper; Efron and Tibshirani (1993, chap. 18) give a comprehensive presentation. Empirical tests (Ague, unpub. data) indicate that calibration should be used if the number of samples in either the protolith or altered sample sets is less than about 15. The

reader is referred to Efron and Tibshirani (1993, chap. 25) for a detailed discussion of how sample size affects the the accuracy of bootstrap-based confidence intervals. It is important to note that any type of confidence interval calculation method, even the calibrated percentile method, will most likely yield unreliable results for extremely small samples ($N°$ or N' less than about 4). Such small samples are, in most cases, unsuitable for rigorous statistical analysis.

The calibrated percentile interval provides many advantages over the standard intervals based on the normal curve. Consider the 95 percent confidence interval for the K_2O mass change example of Figure 1. This is a small sample problem because $N° = 7$ and $N' = 6$. The upper and lower confidence limits for the standard normal interval were calculated using the familiar:

$$\pm 2\hat{\sigma}_{se}, \tag{24}$$

where $\hat{\sigma}_{se}$ is the estimated standard error (the estimated standard deviation of the mean). The largest possible negative τ^j value, -100 percent, corresponds to total depletion of j from the altered rock. The asymmetry of the bootstrap distribution (Fig. 1) is due, in part, to the -100 percent limit on τ^j values. Note that the standard normal interval fails to capture the asymmetry of the distribution, whereas the calibrated percentile interval does (Fig. 1). Furthermore, the standard normal interval extends to τ^{K_2O} values of -110 percent, which are clearly impossible. The calibrated percentile interval, on the other hand, falls entirely within the allowable range of mass change values (in statistical terms, the calibrated percentile interval is said to be "range preserving"; Efron and Tibshirani, 1993). Moreover, the length of the standard normal interval is too small because normal theory is ill-suited for small sample problems (Student's t distribution provides a better basis for estimating confidence limits in the small sample case; cf. Spiegel, 1961). In sum, the calibrated percentile method provides reliable confidence limits whether the distribution is asymmetric, as is the case for τ^{K_2O}, or follows the normal curve; the method is used throughout the rest of this paper.

The Geochemical Reference Frame

Quantification of open-system mass and volume changes requires that one or more immobile reference species be identified. This task is simplified if four basic types of unsuitable species are eliminated from consideration: (1) species that are concentrated in mineral phases that grew in obvious metasomatic environments, for example, if a rock is cut by an array of hydrothermal quartz veins, then silica was mobile and should not be considered as a reference species; (2) species whose concentrations have large uncertainties as a result of analytical problems; (3) species whose concentrations in the protolith are known to be highly variable; and (4) volatile species such as H_2O and CO_2. Volatiles are the agents of mass and heat transport in hydrothermal systems and, therefore, are poor candidates for the reference frame. With these four constraints in mind, some of the approaches for selecting the correct reference frame are discussed.

The best approach is to establish direct, independent geologic constraints on species immobility. For example, Brimhall et al. (1992) used both scanning electron microscope (SEM) imaging and U/Pb isotope systematics to assess zircon solubility during bauxite formation in Western Australia. Pristine euhedral zircons occur throughout the soil profile that are identical in shape, size, and color to the zircons in the protolith bedrock gneiss. Using the SHRIMP (sensitive high mass resolution ion microprobe; Compston et al., 1984), Brimhall et al. (1992) found that the formation age and lead loss patterns of the euhedral zircons in both the soil and the bedrock were indistinguishable. The SEM and SHRIMP evidence strongly suggests that zircon was insoluble in the pore solutions and establishes that the soils were derived directly from the underlying bedrock gneiss. On this basis, Brimhall et al. (1992) used Zr as the immobile reference species.

In some cases, direct evidence of element immobility is lacking and the choice of the reference frame is instead based on experimental solubility data. The concentrations of certain elements including Zr, Ti, and Al are extremely low in many types of crustal hydrothermal fluids (e.g., Ragnarsdottir and Walther, 1985; Ayers and Watson, 1991, 1993). Thus, for some rocks, these elements are appropriate choices for the geochemical reference frame. On the other hand, hydrothermal veins containing minerals rich in these elements (e.g., rutile, aluminosilicates) are by no means uncommon and demonstrate that many of the elements often assumed to be immobile can be mobile, at least over millimeter- to centimeter-length scales, under appropriate circumstances. For example, the solubilities of Zr- and Ti-bearing phases are apparently considerable in some halogen-rich fluids and under the P-T conditions prevailing in the deep parts of subduction zones (e.g., Ayers and Watson, 1991; Philippot and Selverstone, 1991).

The third approach, applicable in cases of weak to moderate alteration, is to make use of the mathematical constraints governing the concentration ratios of immobile species (see Woronow and Love, 1990, for a detailed discussion of these constraints). As pointed out by many previous workers, a key constraint is that the ratio $\bar{C}_i°/\bar{C}_i'$ should be the same for all immobile elements (e.g., Grant, 1986; Ague, 1994a). For weak to moderate degrees of alteration, many or most of the constituents may remain immobile, or nearly so. Thus, the reference frame can be defined on the basis of the maximum number of elements that have compatible $\bar{C}_m°/\bar{C}_m'$ ratios. This is the principle behind the isocon method of Grant (1986) and the weighted least-squares isocon method of Baumgartner and Olsen (1995). A potential pitfall of this approach is that mobile species that undergo comparable amounts of mass transfer will also have comparable $\bar{C}_j°/\bar{C}_j'$ ratios (the subscript j denotes mobile species, see Table 1). If the reference frame is mistakenly constructed using the concentration ratios of the mobile species, then gross errors in estimates of mass and volume change will result. Furthermore, the method is unsuitable for highly altered systems in which most elements were mobile.

If independent geologic evidence can be used to quantify the volume change attending alteration, then the correct reference species ratio can be determined from equation 2. Unambiguous strain markers that rigorously constrain the volume change are, however, rare in practice.

Any of the above four approaches can potentially identify more than one immobile species. The question then arises: which species should be used in the mass balance calculations? Four simple options are presented here. As a starting point, a geometric mean best estimate for the reference species concentration ratio, $\widehat{mr}$, can be calculated using:

$$\widehat{mr} = g_{\hat{r}_i}, \tag{25}$$

where $g_{\hat{r}_i}$ is the geometric mean of the $\hat{r}_i$ ratios. The geometric mean is used here because, in general, it provides better results than the arithmetic mean for ratio quantities (cf. Spiegel, 1961):

Option A. One option is simply to use the species whose $\bar{C}_i^\circ/\bar{C}_i'$ ratio is closest to the mean reference ratio calculated with equation 25.

Option B. If the $\bar{C}_i^\circ/\bar{C}_i'$ ratios of several species are all equally close to the mean ratio (eq 25), then the sum of the concentrations of these species can be used as the reference "species" for the mass balance calculations. For example, consider protolith sample 1 ($n = 1$) in a system comprising SiO_2 (species 1), TiO_2 (species 2), and ZrO_2 (species 3) in which TiO_2, and ZrO_2 are immobile. Prior to summation, the composition is $(c_{1,1}^\circ, c_{1,2}^\circ, c_{1,3}^\circ)$. After summation, the composition $(c_{1,1}^\circ, c_{1,\Sigma}^\circ)$ is obtained, where $c_{1,\Sigma}^\circ$ is the concentration sum for protolith sample 1:

$$c_{1,\Sigma}^\circ = c_{1,2}^\circ + c_{1,3}^\circ = c_{1,TiO_2}^\circ + c_{1,ZrO_2}^\circ. \tag{26}$$

Once all the other protolith and altered rock suite compositions are recast following the same procedure, the bootstrap analysis is carried out exactly as described above using equations 10 to 21. This option has the disadvantage that the reference ratios required for analysis ($\bar{C}_\Sigma^\circ/\bar{C}_\Sigma'$ in eqs 13–15; $\bar{C}_\Sigma^{\circ *}/\bar{C}_\Sigma'^*$ in eqs 19–21) are weighted toward the species with the highest concentrations.

Option C. A third option is to use the species whose C_i°/C_i' ratio has the smallest confidence interval length.

Option D. The geometric mean reference ratio (eq 25) can be used directly in the mass balance equations. The best estimates for mass and volume change ($\hat{T}$, $\hat{\tau}^j$, $\hat{\epsilon}$) are computed by substituting $\widehat{mr}$ for the $\bar{C}_i^\circ/\bar{C}_i'$ terms in equations 13 to 15. The bootstrap analysis requires:

$$\widehat{mr}^* = g_{\hat{r}_i^*}. \tag{27}$$

The bootstrap replicates $\hat{T}^*$, $\hat{\tau}^{j*}$, and $\hat{\epsilon}^*$ are computed by substituting $\widehat{mr}^*$ for the $\bar{C}_i^{\circ *}/\bar{C}_i'^*$ terms in equations 19 to 21. The number of $\hat{r}_i$ should be fairly large (about 5 or greater) in order to provide good confidence limit estimates.

In practice, options A to D usually yield very similar results. If they do not, it may be an indication that one or more of the constituents being used as a reference was really mobile to a significant degree. In such cases, it is best to reexamine the criteria used to select the reference species to see if evidence for element mobility was overlooked.

To summarize, the selection of immobile reference species should be guided by all field, petrographic, thermodynamic, kinetic, isotopic, and mathematical constraints available for a particular problem. Reference frame selection is examined further in the following section.

Application: Deep Crustal Hydrothermal Alteration of Marble

Introduction

We apply our approach to the controversial problem of whether significant volume strain and transport of nonvolatile elements occurs as a result of regional metamorphism and fluid flow in orogenic belts.

Ague (1994a, 1994b, 1995) presented evidence that amphibolite facies metamorphism of pelitic schist can be accompanied by significant, previously unrecognized, chemical mass transfer and mineralogic alteration. The study area was the Wepawaug Schist, Connecticut, which is characterized by a well-developed sequence of Barrovian isograds (Fig. 2; see Fritts, 1963, 1965a, b). Metasomatism in pelitic schist was closely related to synmetamorphic fluid flow through fractures (the fractures are now quartz veins). Vein abundance

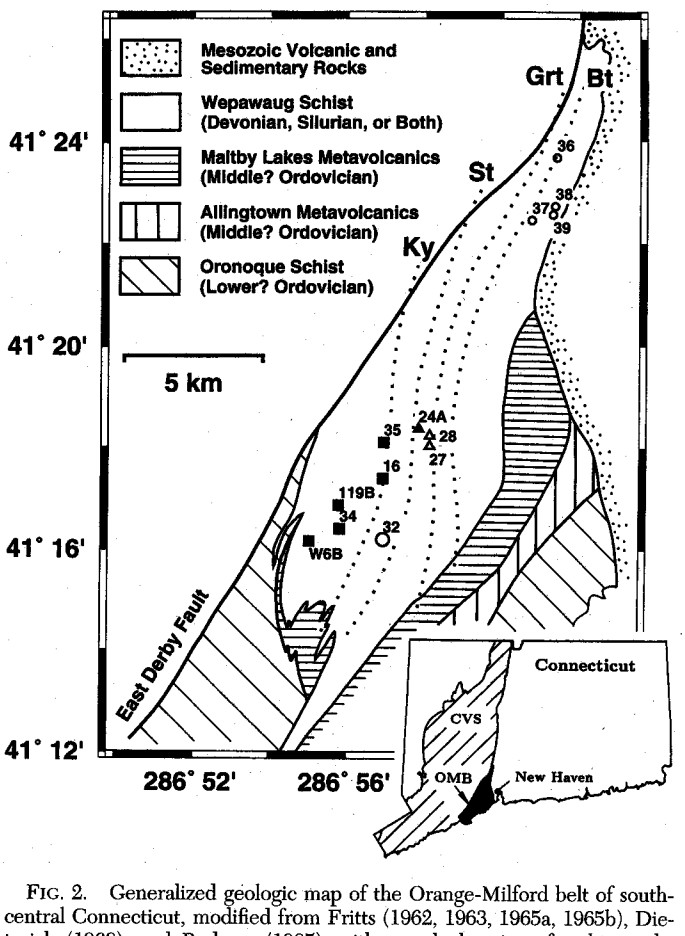

FIG. 2. Generalized geologic map of the Orange-Milford belt of south-central Connecticut, modified from Fritts (1962, 1963, 1965a, 1965b), Dieterich (1968), and Rodgers (1985), with sample locations for this study. Isograd positions modified from Fritts (1963, 1965a, 1965b) by Ague (1994a). Bt = biotite isograd, Grt = garnet isograd, Ky = kyanite isograd, St = staurolite isograd. Symbols for samples: small circles = chlorite zone, triangles = garnet zone, large circles = staurolite zone, squares = kyanite zone: open symbols = parent marbles containing ankerite and muscovite, filled symbols = altered rocks. The position of the Orange-Milford belt (OMB) in the Connecticut Valley synclinorium (CVS) is shown on the inset location map.

increases systematically from 2 to 4 vol percent in the chlorite zone to 20 to 30 percent in the kyanite zone. Fluid infiltration led to the growth of chemically and isotopically altered selvages adjacent to many amphibolite facies veins (Ague, 1994b). The reactions that proceeded during selvage formation commonly resulted in losses of alkali metals (particularly Na), alkaline earth metals, and P and gains of Cu, Mn, and Zn. In addition, some schists gained K and Ba. Petrologic relations (Ague, 1994b) and oxygen isotope systematics (van Haren et al., 1996) suggest that formation of the average amphibolite facies vein required flow of large amounts of H_2O-rich fluid down regional temperature gradients (time-integrated flux $\sim 3 \times 10^5$ m^3 fluid m^{-2}). Mass exchange between infiltrating fluids and schist occurred on 1- to 10-cm-length scales perpendicular to fractures, and at the regional scale along fracture flow paths.

Marble beds are intercalated with quartzofeldspathic rocks throughout the Wepawaug Schist (Fritts, 1963, 1965a, b; Hewitt, 1973; Palin, 1992). Marbles potentially provide a comprehensive history of element transport because they are highly reactive recorders of fluid-rock interaction (cf. Rye et al., 1976; Rumble et al., 1982; Tracy et al., 1983; Bickle and Baker, 1990; Valley et al., 1990; Baumgartner and Ferry, 1991; Dipple and Ferry, 1992; Ferry, 1992, 1995; Lasaga and Rye, 1993; Nabelek, 1993; Bowman et al., 1994). Previous petrologic and isotopic studies indicated that upper greenschist facies and amphibolite facies metamorphism of the Wepawaug marbles was accompanied by substantial infiltration of H_2O-rich fluid (Hewitt, 1973; Tracy et al., 1983; Palin, 1992). Dehydrating pelitic rocks and outgassing magmas were the probable sources of most of the fluid (van Haren et al., 1996); the specific sources and flow pathways for the fluids that produced the alteration of marbles described herein remain to be established. Time-integrated fluid fluxes through some of the marble units may have been locally as large as $\sim 10^5$ m^3 m^{-2} (Palin, 1992; Palin and Rye, 1992). Palin (1992) calculated that interconnected pore fluids were present for only $\sim 10^3$ yr or less during peak metamorphism of the marbles. If fluid flow was episodic, then the total duration of flow may have been longer than 10^3 yr. Infiltration occurred both pervasively (i.e., throughout the rock along grain boundaries) and along macroscopic fractures (now represented by quartz veins). Tracy et al. (1983) found that synamphibolite facies infiltration along a fracture resulted in decreases in $\delta^{18}O$, $\delta^{13}C$, K/Al, Na/Al, Ca/Al, Mg/Fe, and volume in a sample of marble adjacent to the fracture.

In this paper we quantify the amounts of volume change and mass transfer of volatile and nonvolatile constituents that occurred during infiltration of the marble beds under upper greenschist facies and amphibolite facies conditions. Our goal is to obtain a more complete understanding of element mobility in common rock types during regional metamorphism. In so doing, we provide an example application of the bootstrap-based statistical methods described above. The marble beds can be traced upgrade across the Wepawaug and therefore represent an ideal opportunity to assess metamorphic mass transfer.

The Wepawaug metacarbonates have been termed "impure marbles" (e.g., Tracy et al., 1983) because their sedimentary precursors contained substantial quartz, clays, and organic matter. For simplicity, however, we refer to the metacarbonates as "marbles."

Geologic setting and mineral reactions

The Wepawaug Schist forms part of the Orange-Milford belt of south-central Connecticut (Rodgers, 1985) and consists mainly of metamorphosed pelites and psammites (Fig. 2). Fritts (1962) suggested that sediment deposition occurred during the Siluro-Devonian. Metacarbonate beds comprise about 5 to 10 vol percent of the entire rock mass and range in thickness from the centimeter to the meter scale. Peak metamorphic temperatures ranged from ~400° to ~600°C from the chlorite to the kyanite zone, and peak pressures were $\sim 0.8 \pm 0.1$ GPa (Ague, 1994b; van Haren et al., 1996). The regional structural and stratigraphic relations discussed by Dieterich (1968) and the more recent geochronologic results of Palin and Seidemann (1990), Lanzirotti et al. (1995), and Lanzirotti and Hanson (1996) suggest that metamorphism and deformation occurred during the Acadian orogeny (~420–360 Ma; Gates, 1975; Osberg et al., 1989; Armstrong et al., 1992).

The general sequence of metacarbonate mineral assemblages that developed during progressive metamorphism was described by Hewitt (1973) and Palin (1992); their results are summarized here. The assemblage sequence is similar to that observed for metacarbonates elsewhere in New England, such as in the Waits River Formation of Vermont (e.g., Ferry, 1992; Léger and Ferry, 1993).

Lower and middle greenschist facies marbles consist mostly of calcite, ankerite, muscovite, and quartz. The modal abundances of these minerals vary little from one marble bed to the next (Hewitt, 1973) and, therefore, marble bulk compositions are relatively constant throughout the low-grade metamorphic zones. In the upper greenschist and lower amphibolite facies, biotite was produced by the generalized reaction: muscovite + 3 dolomite + 2 quartz → biotite + anorthite + 2 calcite + $4CO_2$. Between the garnet and kyanite isograds, amphibole and K feldspar were produced: 5 biotite + 6 calcite + 24 quartz → 3 amphibole + 5 K feldspar + $6CO_2$ + $2H_2O$. Zoisite and diopside also formed in upper greenschist and amphibolite facies rocks by reactions such as: 3 anorthite + calcite + H_2O → 2 zoisite + CO_2, biotite + 3 calcite + 6 quartz → 3 diopside + K feldspar + $3CO_2$ + H_2O, and amphibole + 3 calcite + 2 quartz → 5 diopside + H_2O + CO_2. Diopside and zoisite growth required extensive infiltration of H_2O-rich fluid (Hewitt, 1973; Tracy et al., 1983; Palin, 1992). Sphene probably formed from rutile by reactions such as: calcite + quartz + rutile → sphene + CO_2.

Samples and methods

We studied hand samples taken from the interior portions of marble beds away from contacts with quartzofeldspathic rocks. Mineral assemblages are listed in Table 3.

Marbles that contain ankerite and muscovite (cal-ank-ms marbles) underwent the least fluid-rock interaction and provide a protolith baseline for assessing mass and volume changes in the more heavily infiltrated rocks. The sample suite of cal-ank-ms marbles (Table 3) comprises four rocks from the chlorite zone (JvH-W-36, -37, -38, -39), two from

TABLE 3. Mineral Assemblages

Sample no.	Zone	Cal	Ank	Ms	Bt	Chl	Qtz	Pl	Kfs	Di	Amp	Zo-Czo	Grt	Rt	Ilm	Po	Py	Ccp	Spn	Gr
Cal-ank-ms marbles																				
27	Grt	×	×	×	×	tr	×	–	–	–	–	–	–	×	–	×	–	–	–	×
28	Grt	×	×	×	×	tr	×	×	–	–	–	–	–	×	–	–	–	–	–	×
32	St	×	×	×	×	×	×	–	–	–	–	–	–	×	tr	×	–	–	–	×
36	Chl	×	×	×	–	tr	×	–	–	–	–	–	–	×	–	–	×	tr	–	×
37	Chl	×	×	×	–	–	×	–	–	–	–	–	–	×	–	–	×	–	–	×
38	Chl	×	×	×	–	–	×	–	–	–	–	–	–	×	–	–	×	–	–	×
39	Chl	×	×	×	–	–	×	–	–	–	–	–	–	×	–	–	×	–	–	×
Altered marbles																				
16	Ky	×	–	–	–	–	×	–	×	×	–	×	–	–	–	–	–	–	×	×
24A	Grt	×	–	–	×	–	tr	–	–	×	×	×	–	–	–	–	–	–	×	×
34	Ky	×	–	–	–	–	tr	–	–	×	×	×	–	–	–	–	–	–	×	×
35	Ky	×	–	–	–	–	tr	–	–	×	×	×	–	–	–	–	–	–	×	×
119B	Ky	×	–	–	–	–	–	–	–	×	×	×	–	–	–	–	–	–	×	×
W6B	Ky	×	–	–	×	–	×	–	tr	–	×	tr	×	–	×	×	–	–	–	×

× = present, – = absent, tr = trace

Abbreviations: Cal = calcite, Ank = ankerite, Ms = muscovite, Bt = biotite, Chl = chlorite, Qtz = quartz, Pl = plagioclase, Kfs = K feldspar, Di = diopside, Amp = calcic amphibole, Zo-Czo = zoisite ± clinozosite, Grt = garnet, Rt = rutile, Ilm = ilmenite, Po = pyrrhotite, Py = pyrite, Ccp = chalcopyrite, Spn = sphene, Gr = graphite

Metamorphic zones: Grt = garnet, St = staurolite, Chl = chlorite, Ky = kyanite

the garnet zone (JvH-W-27, -28), and one from the staurolite zone (JvH-W-32).

With increasing degrees of metamorphism and fluid-rock interaction, ankerite and muscovite were destroyed and assemblages containing various combinations of calcic amphibole, diopside, zoisite (sometimes accompanied by clinozoisite), and garnet were produced (Hewitt, 1973; Palin, 1992). We considered samples that contain zoisite ± diopside ± garnet and that lack ankerite and muscovite collectively as altered marbles (Table 3). Six such samples were studied, one from the garnet zone (JvH-W-24A) and five from the kyanite zone (JvH-W-16, -34, -35; JAW-119; W-6B).

Most whole-rock major, minor, and trace element chemical analyses were done using X-ray fluorescence (XRF) methods by X-ray Assay Laboratories, Ltd., Don Mills, Ontario, Canada (Table 2). The accuracy and reproducibility of results from this laboratory are documented elsewhere (Ferry, 1988; Ague, 1994a). The concentrations of Ba and Rb in samples JvH-W-34, JvH-W-35, and JAW-119B are below analytical detection limits for the XRF procedure (50 ppm for Ba; 10 ppm for Rb). The Ba and Rb concentrations in these three samples were determined by Activation Laboratories Ltd. of Ancaster, Ontario, Canada, using a highly sensitive inductively coupled plasma-mass spectrometry (ICP-MS) technique that has detection limits of 0.01 ppm for Ba and Rb. Rock grain densities (ρ_g, rock density on a porosity-free basis) were measured on pulverized samples using a Micromeritics 1305 manual gas pycnometer at Yale University. The measurements are accurate to within ± 0.005 g cm^{-1} (Ague, 1994a). Because the porosity of in-situ deep crustal rocks is probably small ($<\sim 1\%$), we used grain density to approximate bulk density when calculating volume strain (cf. Ague, 1994a, p. 1041).

The mass balance calculations were done using oxide weight percents; treating oxygen and each cation as separate entities yields nearly identical results.

Construction of calibrated percentile intervals is computationally intensive; 5,000 bootstrap samples were generated to determine the bootstrap distributions for the variables of interest (e.g., mass changes, Fig. 1). For each of these samples, 5,000 more were generated for the calibration, making the total number of samples = 5,000 · 5,000 = 25,000,000. This computational load, while considerable, poses no problems for modern computer workstations.

Geochemical reference frame

Several constituents were eliminated as reference frame candidates. Silica was eliminated because quartz veins comprise a significant proportion of the amphibolite facies rocks (Ague, 1994b). Ti was eliminated because some veins that cut marbles contain rutile and, more rarely, sphene. Loss on ignition (L.O.I.) was eliminated because it reflects primarily the amount of the volatile species CO_2 and H_2O in the rock.

Of the remaining constituents, a large number (12; Al_2O_3, Fe_2O_3, MgO, MnO, CaO, Na_2O, P_2O_5, ZrO_2, ZnO, NiO, Nb_2O_5, and CoO) have very similar r_m ratios whose 95 percent confidence intervals mutually overlap (Fig. 3). Metasomatism is unlikely to have produced such similar ratios for such a broad and geochemically diverse range of species. Consequently, these 12 species probably underwent relatively little or perhaps no mass transfer during metamorphism and, therefore, can be used to define the geochemical reference frame. For the rest of the discussion, the subscript i (the reference species subscript, Table 1) is used for these 12 species. A simple but rigorous way to proceed is first to compute the best estimate of the reference ratio, $\hat{mr}$ (eq 25), using these 12 $\hat{r}_i$ values. The value of $\hat{mr}$ is 0.74; $\hat{r}_{ZrO_2}$ (=0.74), $\hat{r}_{ZnO}$ (=0.74), $\hat{r}_{NiO}$ (=0.73), $\hat{r}_{Nb_2O_5}$ (=0.75), and $\hat{r}_{CoO}$ (=0.73)

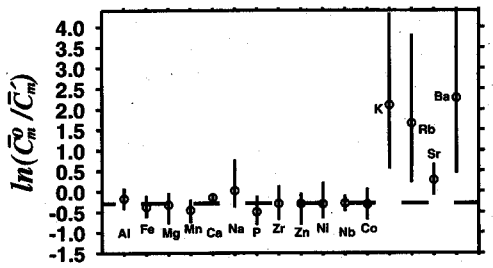

FIG. 3. Reference frame selection. Natural logarithms of the ratio $\hat{\tau}_m = \bar{C}^o_m/\bar{C}'_m$; 95 percent confidence intervals denoted by vertical black bars. Note that 12 constituents (Al_2O_3, Fe_2O_3, MgO, MnO, CaO, Na_2O, P_2O_5, ZrO_2, ZnO, NiO, Nb_2O_5, and CoO) have very similar ratios whose 95 percent confidence limits mutually overlap. The best estimate of the reference ratio, $\hat{mr}$ (eq 25), is based on the concentration systematics of these species and is shown with the horizontal dashed line. Because $\hat{mr}$ is less than 1, overall mass loss occurred during alteration ($\hat{mr} = 0.74$; $ln\ \hat{mr} = -0.30$). The concentration ratios for K_2O, Rb_2O, SrO, and BaO are all much greater that $\hat{mr}$, which suggests that mass loss of these constituents occurred during alteration.

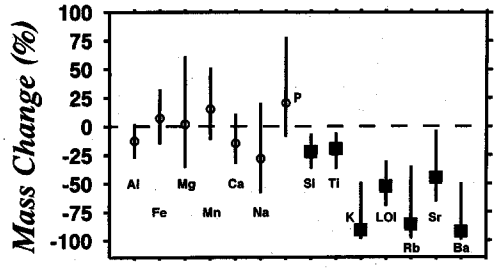

FIG. 4. Mass changes (in %; eqs 14, 20) for hydrothermally altered marble relative to cal-ank-ms marble; 0 mass change denoted by horizontal dashed line. Positive mass changes indicate mass gain, negative mass changes indicate mass loss. The 95 percent confidence intervals is shown with solid black bars. Mass changes for constituents whose confidence intervals do not overlap with the 0 percent mass change line are interpreted to be statistically significant at the 95 percent confidence level. Filled squares are the best estimates for mass changes of mobile constituents SiO_2, TiO_2, K_2O, L.O.I. (which approximates total $H_2O + CO_2$ content), Rb_2O, SrO, and BaO. Open circles are best estimates of mass changes for species whose 95 percent confidence intervals overlap with the 0 mass change line; mass changes for these elements are not significant at the 95 percent confidence level.

are all nearly identical to this ratio. Thus, we selected Zr, Zn, Ni, Nb, and Co as the reference immobile elements and used reference frame option B described above to estimate mass and volume changes. We note that the other options yield very similar estimates of mass and volume change.

Some important conclusions can be drawn by inspection of the concentration ratio systematics. For example, because $\hat{mr}$ is less than one (Fig. 3), overall rock mass loss occurred during the alteration (cf. eq 1). If the concentration ratio for a chemical constituent is significantly greater than $\hat{mr}$, as is the case for K_2O (Fig. 3), then mass loss of the constituent is indicated; a ratio less than $\hat{mr}$ indicates mass gain.

Results: Mass and volume changes

Our calculations indicate that altered marbles lacking ankerite and muscovite lost statistically significant (95% confidence) amounts of volatiles (approximated by L.O.I.), Si, Ti, K, Rb, Sr, and Ba relative to cal-ank-ms marbles (Fig. 4; Table 4). If other elements were also mobile, then variability due to factors such as protolith heterogeneity has obscured the mass change signal. The depletion of K, Rb, and Ba was particularly severe—$\hat{\tau}^{K_2O}$, $\hat{\tau}^{Rb_2O}$, and $\hat{\tau}^{BaO}$ are −91, −86, and −92 percent, respectively (Table 4). Note that some of the mass change distributions are strongly non-normal (e.g., $\hat{\tau}^{K_2O}$; Figs. 1 and 4). The bootstrap-based statistical approach used in this paper gives rigorous confidence intervals for these distributions, whereas standard methods based on the normal curve will fail.

The total mass change relative to the suite of cal-ank-ms marbles was about −27 percent (Table 4). Thus, on average, 1 kg of cal-ank-ms marble lost about 270 g. The bulk of the lost mass was volatiles (~140 g kg^{-1}), SiO_2 (~60 g kg^{-1}), and K_2O (~15 g kg^{-1}) (Table 4).

Mass loss and rock density changes contributed to the overall rock volume change. Grain density increased significantly during metamorphism. The mean grain densities of the cal-ank-ms and altered marble suites are 2.79 [2.76, 2.84] and 3.01 [2.90, 3.14], respectively (bracketed numbers are the end points of the 95% confidence intervals). Using equation 15, the best estimate of volume strain is about −32%—in other words, 100 cm^3 of cal-ank-ms marble lost, on average, about 32 cm^3 of volume (Table 4).

Infiltration of water-rich fluids drove devolatilization reactions during prograde metamorphism (Hewitt, 1973; Tracy et al., 1983; Palin, 1992). Thus, if the physicochemical changes observed for altered marble are the result of fluid infiltration, then they should correlate with the degree of devolatilization. A simple index of devolatilization extent is $c_{n,\text{L.O.I.}}/c_{n,\Sigma}$, where n is the sample number and Σ is the concentration sum for the reference species. Note that a ratio quantity must be used because compositions provide information only about the relative proportions of constituents. The $c_{n,\text{L.O.I.}}/c_{n,\Sigma}$ ratio gets smaller with increasing loss of volatiles.

TABLE 4. Mass and Volume Changes

	Percent	g kg^{-1}
SiO_2	−22 [−37, −7]	-6.2×10^1 [-1.0×10^2, -2.0×10^1]
TiO_2	−20 [−37, −6]	-4.7×10^{-1} [-8.9×10^{-1}, -1.4×10^{-1}]
K_2O	−91 [−99, −50]	-1.5×10^1 [-1.6×10^1, -8.1×10^0]
L.O.I.	−52 [−70, −30]	-1.4×10^2 [-1.9×10^2, -8.2×10^1]
L.O.I.[1]	−58 [−73, −39]	-1.6×10^2 [-2.0×10^2, -1.1×10^2]
Rb_2O	−86 [−99, −35]	-4.8×10^{-2} [-5.5×10^{-2}, -1.9×10^{-2}]
SrO	−45 [−66, −3]	-5.4×10^{-1} [-7.9×10^{-1}, -4.1×10^{-2}]
SrO[1]	−54 [−72, −27]	-7.1×10^{-1} [-9.5×10^{-1}, -3.6×10^{-2}]
BaO	−92 [−99, −50]	-2.1×10^{-1} [-2.3×10^{-1}, -1.2×10^{-1}]
Rock mass	−27 [−43, −12]	-2.7×10^2 [-4.3×10^2, -1.2×10^2]
Volume strain	−32 [−48, −17]	

Mass and volume changes computed for altered marbles relative to all cal-ank-ms marbles unless otherwise noted; g kg^{-1} = mass change in grams per kilogram of cal-ank-ms marble; Braketed numbers are end points of 95 percent confidence intervals

[1] Mass changes computed for altered marbles relative to chlorite zone cal-ank-ms marbles.

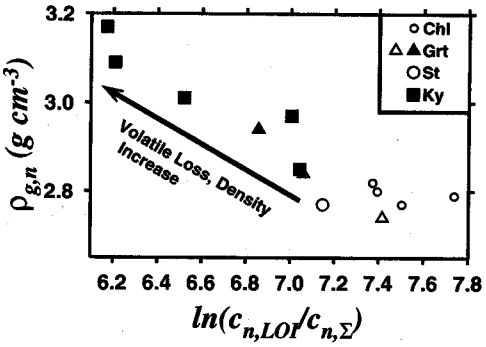

FIG. 5. Rock grain density for each sample, n, shown as function of devolatilization extent ($c_{n,\text{L.O.I}}/c_{n,\Sigma}$). Open symbols = cal-ank-dol marbles, filled symbols = altered rocks. Metamorphic zones: Chl = chlorite, Grt = garnet, St = staurolite, Ky = kyanite. Note that grain density of the altered rocks increases with increasing volatile loss.

The linkages between fluid infiltration, devolatilization, and rock physical properties are well illustrated by grain density systematics. The grain density of the altered marbles increases with increasing degrees of devolatilization (Fig. 5), reflecting the progressive growth of high-density phases like diopside, zoisite, clinozoisite, and amphibole at the expense of carbonates, quartz, plagioclase, and muscovite.

Element mobility was investigated further by examining the ratio $c_{n,j}/c_{n,\Sigma}$ as a function of devolatilization extent. This ratio gets smaller with progressive loss of j. K, Rb, and Ba mass loss for the altered rocks increases with increasing volatile loss (Fig. 6A, B, C). Loss of Sr from the altered rocks also increases with increasing devolatilization (Fig. 6D). Some of the cal-ank-ms marbles from the garnet and staurolite zones, however, also appear to have lost Sr (Fig. 6D). Thus, Sr may have been lost progressively throughout the metamorphism, even from rocks that retain the ankerite + muscovite assemblage. The data of Figure 6 strongly suggest that loss of alkali and alkaline earth metals was directly related to devolatilization. Mass loss systematics for Si and Ti are less regular than those for the alkali and alkaline earth metals. The most volatile-depleted rocks have the lowest $c_{n,\text{SiO}_2}/c_{n,\Sigma}$ and $c_{n,\text{TiO}_2}/c_{n,\Sigma}$ ratios, however, which suggests that volatile loss and Si and Ti mass transfer were related (Fig. 7).

The relations of Figures 5 to 7 suggest that cal-ank-ms marbles from the garnet and staurolite zones have $c_{n,\text{L.O.I}}/c_{n,\Sigma}$ values that are lower than those of cal-ank-ms marbles from the chlorite zone, although the number of data is limited. Consequently, the cal-ank-ms marbles probably lost volatiles progressively during the metamorphism (cf. Palin, 1992). As a result, the L.O.I. mass change for altered marbles (those lacking ankerite and muscovite) relative to chlorite zone cal-ank-ms marbles (−58% [−73%, −39%]) is slightly greater than the L.O.I. mass change computed relative to the entire suite of cal-ank-ms marbles (−52% [−70%, −30%]; Table 4). Similar relations hold true for Sr, which was also probably lost progressively during prograde metamorphism (Fig. 6; Table 4).

It is interesting to note that most of the cal-ank-ms marbles contain either pyrite (chlorite zone) or pyrrhotite (garnet and staurolite zones), whereas only one of the altered marbles contains a sulfide phase (pyrrhotite, Table 3). Although sufur concentrations were not determined in this study, these mineralogical relations (Table 3) strongly suggest that sulfur was lost from the altered marbles.

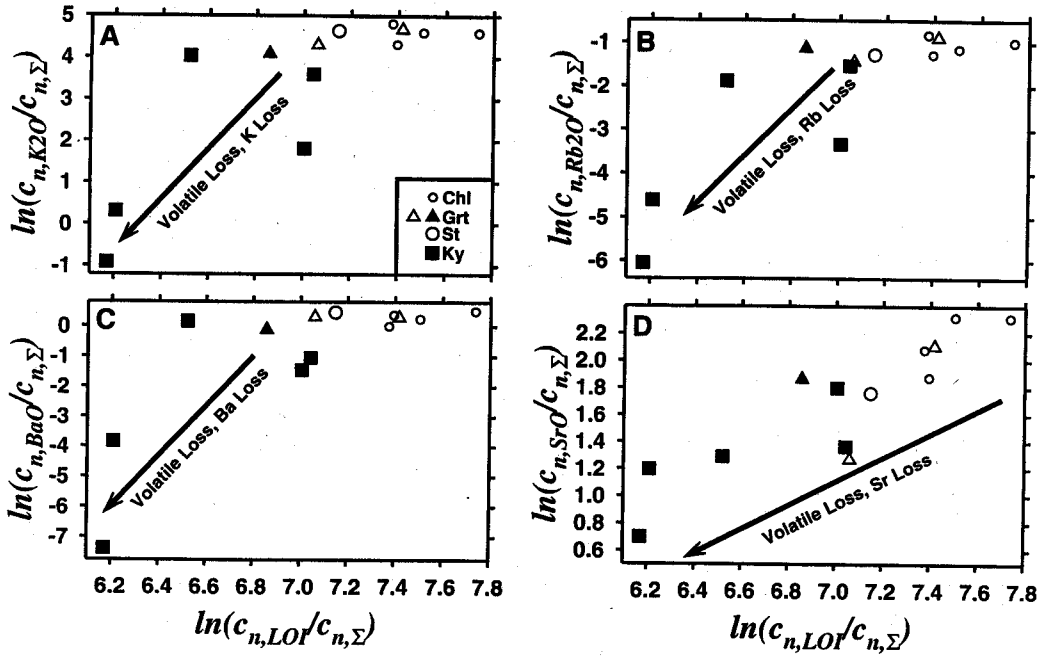

FIG. 6. Indices of mass change ($c_{n,j}/c_{n,\Sigma}$) as functions of devolatilization extent ($c_{n,\text{L.O.I}}/c_{n,\Sigma}$) for each sample, n. Open symbols = cal-ank-ms marbles, filled symbols = altered rocks. Metamorphic zones: Chl = chlorite, Grt = garnet, St = staurolite, Ky = kyanite. A. ln ($c_{n,\text{K}_2\text{O}}/c_{n,\Sigma}$) versus ln ($c_{n,\text{L.O.I}}/c_{n,\Sigma}$). Note increasing potassium loss with increasing volatile loss for the altered rocks. B. ln ($c_{n,\text{Rb}_2\text{O}}/c_{n,\Sigma}$) versus ln ($c_{n,\text{L.O.I}}/c_{n,\Sigma}$). C. ln ($c_{n,\text{BaO}}/c_{n,\Sigma}$) versus ln ($c_{n,\text{L.O.I}}/c_{n,\Sigma}$). D. ln ($c_{n,\text{SrO}}/c_{n,\Sigma}$) versus ln ($c_{n,\text{L.O.I}}/c_{n,\Sigma}$).

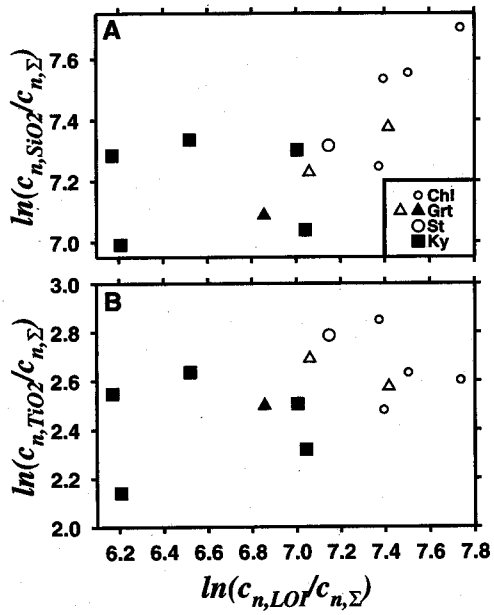

FIG. 7. Indices of mass change for (A) SiO_2 and (B) TiO_2 as functions of devolatilization extent ($c_{n,L.O.I}/c_{n,\Sigma}$) for each sample, n. Open symbols = cal-ank-ms marbles, filled symbols = altered rocks; metamorphic zones: Chl = chlorite, Grt = garnet, St = staurolite, Ky = kyanite.

Evidence for mobility of nonvolatile elements during Acadian metamorphism of marbles has also been found elsewhere in New England. For example, Ferry (1982) found that K and Na were progressively removed from marbles of the Waterville Formation, Maine, with increasing metamorphic grade. Léger and Ferry (1993) reported that some amphibolite facies (diopside zone) marbles of the Waits River Formation, Vermont, underwent extreme alkali depletion. These results, coupled with our own, strongly suggest that mass transfer of nonvolatile elements (particularly alkali metals) was relatively common during amphibolite and upper greenschist facies Acadian metamorphism.

Discussion and Conclusions

We present a computer-based, statistically rigorous approach for determining likely errors on best estimates of mass and volume changes in metasomatic systems. The FORTRAN 77 computer software that performs the calculations described herein is available from the senior author.

Application of our approach indicates that marble beds of the Wepawaug Schist, Connecticut, which contain zoisite ± diopside ± garnet lost significant volume and mass as a result of devolatilization attending infiltration of H_2O-rich fluids during upper greenschist facies and amphibolite facies metamorphism. Most of the lost volatiles (dominantly CO_2 and H_2O) were probably transported out of the rock mass entirely at the regional scale because quartzofeldspathic rocks and veins throughout the upper greenschist facies and amphibolite facies lack carbonate minerals.

Our analysis also indicates that Si, Ti, K, Rb, Sr, and Ba were lost from the marble beds. Sinks for the K, Rb, Sr, and Ba have yet to be identified, but the synmetamorphic quartz veins that cut the marbles are probable sinks for some or all of the lost Si and Ti. Si, Ti, K, Rb, Sr, and Ba must have been transported over minimum-length scales on the order of typical hand sample size; maximum-length scales remain to be determined. For example, the elements may have been transported locally into adjacent quartzofeldspathic beds by diffusion. On the other hand, they may have been transported out of the rock mass entirely at the regional scale by advective fluid flow. Regional mobility of K could have particularly important consequences for the thermal evolution of orogenic belts because radioactive decay of ^{40}K is a significant source of thermal energy in the crust. Our results, therefore, provide impetus for future studies aimed at determining the nature and extent of pervasive and channelized fluid flow regimes and the roles of advection, diffusion, and hydrodynamic dispersion in producing chemical alteration and controlling mineral reaction histories. Important challenges that remain are to identify the crustal hydrologic pathways by which deep metamorphic fluids communicate with the middle and upper crust, and the contribution that metamorphic fluids make to overall element budgets and hydrothermal alteration in shallow ore-forming systems.

Acknowledgments

We thank M.T. Brandon, G.H. Brimhall, J.M. Palin, and D.M. Rye for discussions; and two *Economic Geology* referees for thoughtful reviews. Financial support from National Science Foundation grants EAR-9106652, EAR-9118006, and EAR-9405889 is gratefully acknowledged.

March 6, November 1, 1996

REFERENCES

Ague, J.J., 1994a, Mass transfer during Barrovian metamorphism of pelites, south-central Connecticut, I: Evidence for composition and volume change: American Journal of Science, v. 294, p. 989–1057.

—— 1994b, Mass transfer during Barrovian metamorphism of pelites, south-central Connecticut, II: Channelized fluid flow and the growth of staurolite and kyanite: American Journal of Science, v. 294, p. 1061–1134.

—— 1995, Mass transfer during Barrovian metamorphism of pelites, south-central Connecticut—reply: American Journal of Science, v. 295, p. 1025–1033.

Ayers, J.C., and Watson, E.B., 1991, Solubility of apatite, monazite, zircon, and rutile in supercritical aqueous fluids with implications for subduction zone geochemistry: Royal Society of London Philosophical Transactions, sec. A, v. 335, p. 365–375.

—— 1993, Rutile solubility and mobility in supercritical aqueous fluids: Contributions to Mineralogy and Petrology, v. 114, p. 321–330.

Aitchison, J., 1986, The statistical analysis of compositional data: London, Chapman and Hall, 416 p.

—— 1989, Measures of location of compositional data sets: Mathematical Geology, v. 21, p. 787–790.

Armstrong, T.R., Tracy, R.J., and Hames, W.E., 1992, Contrasting styles of Taconian, eastern Acadian and western Acadian metamorphism, central and western New England: Journal of Metamorphic Geology, v. 10, p. 415–426.

Baumgartner, L.P., and Ferry, J.M., 1991, A model for coupled fluid flow and mixed-volatile mineral reactions with applications to regional metamorphism: Contributions to Mineralogy and Petrology, v. 106, p. 273–285.

Baumgartner, L.P., and Olsen, S.N., 1995, A least-squares approach to mass transport calculations using the isocon method: ECONOMIC GEOLOGY, v. 90, p. 1261–1270.

Bickle, M.J., and Baker, J., 1990, Advective-diffusive transport of isotopic fronts: An example from Naxos, Greece: Earth and Planetary Science Letters, v. 97, p. 78–93.

Bowman, J.R., Willett, S.D., and Cook, S.J., 1994, Oxygen isotopic transport

and exchange during fluid flow; one-dimensional models and applications: American Journal of Science, v. 294, p. 1–55.
Brady, J.B., 1988, The role of volatiles in the thermal history of metamorphic terranes: Journal of Petrology, v. 29, p. 1187–1213.
Brimhall, G.H, and Dietrich, W.E., 1987, Constitutive mass balance relations between chemical composition, volume, density, porosity, and strain in metasomatic hydrochemical systems: Results on weathering and pedogenesis: Geochimica et Cosmochimica Acta, v. 51, p. 567–587.
Brimhall, G.H, Lewis, C.J., Ague, J.J., Dietrich, W.E., Hampel, J., Teague, T., and Rix, Peter, 1988, Metal enrichment in bauxites by deposition of chemically mature aeolian dust: Nature, v. 333, p. 819–824.
Brimhall, G.H, Chadwick, O.A., Lewis, C.J., Compston, W., Williams, I.S., Danti, K.J., Dietrich, W.E., Power, M.E., Hendricks, D., and Bratt, J., 1992, Deformational mass transport and invasive processes in soil evolution: Science, v. 255, p. 695–702.
Chamberlain, C.P., and Rumble, D., 1988, Thermal anomalies in a regional metamorphic terrane: An isotopic study of the role of fluids: Journal of Petrology, v. 29, p. 1215–1232.
Chayes, F., 1960, On correlation between variables of constant sum: Journal of Geophysical Research, v. 65, p. 4185–4193.
Compston, W., Williams, C.J., and Meyer, J., 1984, U-Pb geochronology of zircons from lunar breccia 73217 using a sensitive high mass-resolution ion microprobe: Journal of Geophysical Research, v. 89, supp. B, p. 525–534.
Dieterich, J.H., 1968, Sequence and mechanics of folding in the area of New Haven, Naugatuck, and Westport, Connecticut: Unpublished Ph.D. thesis, Yale University, New Haven, 153 p.
Dipple, G.M., and Ferry, J.M., 1992, Fluid flow and stable isotopic alteration in rocks at elevated temperatures with applications to metamorphism: Geochimica et Cosmochimica Acta, v. 56, p. 3539–3550.
Efron, B., 1979, Bootstrap methods: Another look at the jackknife: Ann. Statist., v. 7. p. 1–26.
Efron, B., and Tibshirani, R.J., 1993, An introduction to the bootstrap: New York, Chapman and Hall, 436 p.
Ferry, J.M., 1982, A comparative geochemical study of pelitic schists and metamorphosed carbonate rocks from south-central Maine, USA: Contributions to Mineralogy and Petrology, v. 80, p. 59–72.
—— 1988, Infiltration-driven metamorphism in northern New England, USA: Journal of Petrology, v. 29, p. 1121–1159.
—— 1992, Regional metamorphism of the Waits River Formation, eastern Vermont; delineation of a new type of giant metamorphic hydrothermal system: Journal of Petrology, v. 33, p. 45–94.
—— 1995, Overview of the petrologic record of fluid flow during regional metamorphism in northern New England: American Journal of Science, v. 294, p. 905–988.
Fritts, C.E., 1962, Age and sequence of metasedimentary and metavolcanic formations northwest of New Haven, Connecticut: U.S. Geological Survey Professional Paper 450-D, p. 32–36.
—— 1963, Bedrock geology of the Mount Carmel quadrangle, Connecticut: U.S. Geological Survey Quadrangle Map GQ-199.
—— 1965a, Bedrock geologic map of the Ansonia quadrangle, Fairfield and New Haven Counties, Connecticut: U.S. Geological Survey Quadrangle Map GQ-426.
—— 1965b, Bedrock geologic map of the Milford quadrangle, Fairfield and New Haven Counties, Connecticut: U.S. Geological Survey Quadrangle Map GQ-427.
Gates, O., 1975, Geologic map and cross-section of the Eastport quadrangle, Washington County, Maine: Maine Geological Survey, Geology Map Series 3, scale 1:62,500.
Grant, J.A., 1986, The isocon diagram—a simple solution to Gresens' equation for metasomatic alteration: Economic Geology, v. 81, p. 1976–1982.
Gresens, R.L., 1967, Composition-volume relations of metasomatism: Chemical Geology, v. 2, p. 47–65.
Hall, P., 1987, On the bootstrap and likelihood-based confidence intervals: Biometrika, v. 74, p. 481–493.
Hewitt, D.A., 1973, The metamorphism of micaceous limestones from south-central Connecticut: American Journal of Science, v. 273-A, p. 444–469.
Hoisch, T.D., 1991, The thermal effects of pervasive and channelized fluid flow in the deep crust: Journal of Geology, v. 99, p. 69–80.
Lanzirotti, A., and Hanson, G.N., 1996, Geochronology and geochemistry of multiple generations of monazite from the Wepawaug Schist, Connecticut, USA: Implications for monazite stability in metamorphic rocks: Contributions to Mineralogy and Petrology, v. 125, p. 332–340.
Lanzirotti, A., Hanson, G.N., and Smith, R.D., 1995, The Orange-Milford belt of southwestern Connecticut: Identifying unique crustal packages in New England using combined geochemistry, geochronology, and petrology [abs.]: Geological Society of America Abstracts with Programs, v. 27-1, p. 63.
Lasaga, A.C., and Rye, D.M., 1993, Fluid flow and chemical reaction kinetics in metamorphic systems: American Journal of Science, v. 293, p. 361–404.
Léger, A., and Ferry, J.M., 1993, Fluid infiltration and regional metamorphism of the Waits River Formation, northeast Vermont, USA: Journal of Metamorphic Geology, v. 11, p. 3–29.
Loh, W.-Y., 1987, Calibrating confidence coefficients: Journal of the American Statistical Association, v. 82, p. 155–162.
Moss, B.E., Haskin, L.A., Dymek, R.F., and Shaw, D.M., 1995, Redetermination and reevalulation of compositional variations in metamorphosed sediments of the Littleton Formation, New Hampshire: American Journal of Science, v. 295, p. 988–1019.
Nabelek, P.I., 1993, Implications of geochemical fronts in the Notch Peak contact-metamorphic aureole, Utah, USA: Earth and Planetary Science Letters, v. 119, p. 539–559.
Osberg, P.H., Tull, J.F., Robinson, P., Hon, R., and Butler, J.R., 1989, The Acadian orogen, in Hatcher, R.D., Jr., Thomas, W.A., and Viele, G.W., eds., The Appalachian-Ouachita orogen in the United States: Boulder, Colorado, Geological Society of America, Geology of North America, v. F-2, p. 179–232.
Palin, J.M., 1992, Petrologic and stable isotopic studies of the Wepawaug Schist, Connecticut: Unpublished Ph.D. thesis, Yale University, New Haven, 170 p.
Palin, J.M., and Rye, D.M., 1992, Direct comparison of mineralogic and stable isotopic records of metamorphic fluid flow [abs.]: Geological Society of America Abstracts with Programs, v. 24, no. 7, p. A172.
Palin, J.M., and Seidemann, D.E., 1990, Intergranular control of argon and oxygen isotope transport in metamorphic rocks: Implications for cooling-rate studies [abs.]: V.M. Goldschmidt Conference, 2nd, Baltimore, Maryland, Program and Abstracts, p. 71.
Pearson, K., 1897, Mathematical contributions to the theory of evolution. On a form of spurious correlation which may arise when indices are used in the measurement of organs: Royal Society of London Proceedings, v. 60, p. 489–498.
Philippot, P., and Selverstone, J., 1991, Trace-element-rich brines in eclogitic veins: Implications for fluid composition and transport during subduction: Contributions to Mineralogy and Petrology, v. 106, p. 417–430.
Ragnarsdottir, K.V., and Walther, J.V., 1985, Experimental determination of corundum solubilities in pure water between 400–700 degrees C and 1–3 kbar: Geochimica et Cosmochimica Acta, v. 49, p. 2109–2115.
Rodgers, J., 1985, Bedrock geological map of Connecticut: Connecticut Geological and Natural History Survey, Department of Environmental Protection, scale 1:125,000.
Rumble, D., III, Ferry, J.M., Hoering, T.C., and Boucot, A.J., 1982, Fluid flow during metamorphism at the Beaver Brook fossil locality: American Journal of Science, v. 282, p. 886–919.
Rye, R.O., Schuiling, R.D., Rye, D.M., and Jansen, J.B.H., 1976, Carbon, hydrogen and oxygen isotope studies of the regional metamorphic complex at Naxos, Greece: Geochimica et Cosmochimica Acta, v. 40, p. 1031–1049.
Spiegel, M.R., 1961, Theory and problems of statistics: New York, McGraw-Hill, 359 p.
Tracy, R.J., Rye, D.M., Hewitt, D.A., and Schiffries, C.M., 1983, Petrologic and stable-isotopic studies of fluid-rock interactions, south-central Connecticut: I. The role of infiltration in producing reaction assemblages in impure marbles: American Journal of Science, v. 283-A, p. 589–616.
Valley, J.W., Bohlen, S.R., Essene, E.J., and Lamb W., 1990, Metamorphism in the Adirondacks: II. The role of fluids: Journal of Petrology, v. 31, p. 555–596.
van Haren, J.L.M., Ague, J.J., and Rye, D.M., 1996, Oxygen isotope record of channelized and pervasive fluid infiltration during regional metamorphism of pelitic schist, south-central Connecticut, USA: Geochimica et Cosmochimica Acta, v. 60, p. 3487–3504.
Woronow, A., and Love, K.M., 1990, Quantifying and testing differences among means of compositional data suites: Mathematical Geology, v. 22, p. 837–852.